 CMES, vol.6, no.2, pp.123-131, 2004

Fast Multipole Boundary Element Analysis of Corrosion Problems

S.Aoki[1] **K.Amaya**[2] **M.Urago**[3] **and A.Nakayama**[4]

Abstract: The Fast Multipole Boundary Element Method(FMBEM) which is suitable for a large scale computation is applied to corrosion analysis. Many techniques of the FMBEM on the potential problems can be usefully employed. Additionally, some procedures are developed for corrosion analysis. To cope with the non-linearity due to the polarization curve, the Bi-CGSTAB iterative method which is commonly used in the FMBEM is modified. To solve infinite domain problems, the M_0^0 which is obtained naturally in the multipole expansion is conveniently used. A pipe element for the FMBEM is developed. A couple of example problems are solved to show the applicability of the FMBEM to corrosion problems.

keyword: Fast multipole boundary element method (FMBEM), corrosion analysis, large scale computation, infinite domain problem, non-linearity, pipe element.

1 Introduction

The boundary element method (BEM) has extensively developed in recent years [e.g. Aimi, Diligenti, Lunardini and Salvadori (2003), Han and Atluri (2003)], and has become an essential tool in corrosion engineering [Adey, Brebbia and Niku (1990), DeGiorgi, Thomas II, Lucas and Kee (1996), Brichau and Deconinck (1994), Orazem, Esteban, Kennelley and Degerstedt (1997)] as well as in many other engineering fields. Although many problems, such as prediction of galvanic corrosion rate in structures and optimum location of electrodes in a cathodic protection system, can be solved in principle with BEM, there are still many cases where the structure or the protection system is too complicated to be treated in a reasonable CPU time. Various efforts are continued to overcome this difficulty [Aoki, Amaya and Miyasaka (1999)].

It is in general known that the BEM needs calculations of $O(N_0^3)$ (or $O(N_0^{2+\delta})$ $(0 \leq \delta \leq 1)$ for iterative method) and memories of $O(N_0^2)$ for N_0 unknowns[Fujino and Chou (1996)]. On the other hand, the fast multipole boundary element method (FMBEM)[Greengard (1988),Rokhlin (1987),Greengard and Rokhlin (1987), Hayami and Sauter (1997),Nishimura, Yoshida and Kobayashi (1999),Takahashi, Nishimura and Kobayashi (2001)Fukui and Hattori (1998)] can reduce calculations to $O(N_0^{1+\delta})$ and memories to $O(N_0)$.

In this paper, the FMBEM is applied to corrosion analysis. Although it is expected that many results in the above researches on FMBEM can be usefully used , new efforts to cope with the non-linearity due to the polarization curve, to treat the infinite domain problem, and to create a pipe element for FMBEM are still necessary.

2 Basic equation in corrosion problem

The electrolyte domain Ω is assumed to be finite at first, and later the infinite domain will be considered. It is assumed that the surface of electrolyte domain Ω is surrounded by Γ (=Γ_d+Γ_n+Γ_m), where Γ_m is the metal surface, and the potential and current density are prescribed on Γ_d and Γ_n, respectively. The potential ϕ in homogeneous electrolyte domain Ω satisfies the Laplace's equation:

$$\nabla^2\phi = 0 \qquad in \qquad \Omega \tag{1}$$

The boundary conditions are given with

$$\phi = \phi_0 \qquad on \qquad \Gamma_d \tag{2}$$

$$i\left(\equiv \kappa\frac{\partial\phi}{\partial n}\right) = i_0 \qquad on \qquad \Gamma_n \tag{3}$$

$$-\phi = f_m(i) \qquad on \qquad \Gamma_m \tag{4}$$

where ϕ_0 and i_0 are the prescribed values of potential ϕ and current density i , respectively, $\partial/\partial n$ is the outward

[1] Department of Computational Science and Engineering, Toyo University, 2100 Kujirai, Kawagoe, Saitama 350-8585,Japan.
[2] Tokyo Institute of Technology, Ohokayama, Meguro-ku, Tokyo 152-8551, Japan.
[3] Tokyo Institute of Technology, Ohokayama, Meguro-ku, Tokyo.
[4] Tokyo Institute of Technology, Ohokayama, Meguro-ku, Tokyo.

normal derivative, and κ is the conductivity of the electrolyte. The $f_m(i)$ is a non-linear function representing the polarization curve to be determined experimentally. In case where the structure consists of multiple metals, the number of metals is the same as that of polarization curves.

It is noted that the potential ϕ is defined with refering to the metal and has the inverse sign of the potential E employed in the corrosion science in which the potential is defined to a reference electrode such as SCE. The corrosion rate of metal is proportional to the current density i on Γ_m, and it is obtained by solving Equation (1) under the boundary conditions, Equations (2)-(4).

Application of the Green's theorem to Equation (1) yields the following integral equation[Brebbia (1978)].

$$\kappa c(\mathbf{x})\phi(\mathbf{x}) = \int_\Gamma (\phi^*(\mathbf{x},\mathbf{y})i(\mathbf{y}) - i^*(\mathbf{x},\mathbf{y})\phi(\mathbf{y}))\, d\Gamma(\mathbf{y}) \quad (5)$$

where

$$\Gamma = \Gamma_d + \Gamma_n + \Gamma_m \quad (6)$$

$$\phi^*(\mathbf{x},\mathbf{y}) = \frac{1}{4\pi|\mathbf{x}-\mathbf{y}|} \quad (7)$$

$$i^*(\mathbf{x},\mathbf{y}) = \kappa\frac{\partial\phi^*}{\partial n} \quad (8)$$

The $\mathbf{x}$ and $\mathbf{y}$ are the vectors representing points, and $c(\mathbf{x})$ is a known constant related to the geometry of the surface[Brebbia (1978)]. Equation (7) is called the fundamental solution of the Laplace's Equation (1).

Approximation of the values on Γ in Equation (5) by using N constant elements leads to the following discretized equation.

$$\kappa c(\mathbf{x})\phi(\mathbf{x}) = \sum_{j=1}^{N} A_j(\mathbf{x})i_j - \sum_{j=1}^{N} B_j(\mathbf{x})\phi_j \quad (9)$$

where the subscript j represents the quantity related to the j-th element. The coefficients $A_j(\mathbf{x})$ and $B_j(\mathbf{x})$ are given with the following equations.

$$A_j(\mathbf{x}) = \int_{\Gamma_j} \phi^*(\mathbf{x},\mathbf{y})d\Gamma(\mathbf{y}) \quad (10)$$

$$B_j(\mathbf{x}) = \int_{\Gamma_j} i^*(\mathbf{x},\mathbf{y})d\Gamma(\mathbf{y}) \quad (11)$$

The above discussion is for a finite domain Ω. For the case where the domain Ω is infinite, i.e., Ω is surrounded with Γ (See Equation (6)) and the infinite boundary Γ_∞ , Equation (5) is modified as follows,

$$\kappa c(\mathbf{x})\phi(\mathbf{x}) = \int_\Gamma (\phi^*(\mathbf{x},\mathbf{y})i(\mathbf{y}) - i^*(\mathbf{x},\mathbf{y})\phi(\mathbf{y}))\, d\Gamma(\mathbf{y}) + \kappa\phi_\infty \quad (12)$$

where ϕ_∞ is the potential on Γ_∞. For the case where no current flows through Γ_∞, the ϕ_∞ is obtained indirectly by adding following equation to Equation (12).

$$\int_\Gamma i d\Gamma = 0 \quad (13)$$

Equations (12) and (13) are discretized into

$$\kappa c(\mathbf{x})\phi(\mathbf{x}) = \sum_{j=1}^{N} A_j(\mathbf{x})i_j - \sum_{j=1}^{N} B_j(\mathbf{x})\phi_j + \kappa\phi_\infty \quad (14)$$

$$\sum_{j=1}^{N} i_j S_j = 0 \quad (15)$$

where S_j denotes the area of the j-th element.

The boundary conditions, Equations (2)-(4) are discretized similarly. By substituting the discretized boundary conditions into Equation (9) (or (14) and (15) for infinite Ω), and taking $\mathbf{x}$ at the center of each element $\mathbf{x}_i (i = 1, \cdots, N)$, non-linear algebraic equations, the number of which N is equal to that of the unknowns, are obtained. Because N becomes very large for a complicated structure, the multipole expansion is performed for the coefficients $A_j(\mathbf{x})$ and $B_j(\mathbf{x})$, and an iterative method is applied to solve the equations.

3 Multipole expansion of fundamental solution

Before the multipole expansion of coefficients $A_j(\mathbf{x})$ and $B_j(\mathbf{x})$ is performed, the fundamental solution, Equation (7), will be expanded at first. A brief description of the expansion will be given here. Details are referred to the reference[Greengard (1988)].

In general, the multipole expansion of a harmonic function $u(\mathbf{x})$ around the origin O is expressed as

$$u(\mathbf{x}) = \sum_{n=0}^{\infty}\sum_{m=-n}^{n} M_n^m \frac{Y_n^m(\theta,\varphi)}{r^{n+1}} + u_\infty \quad (16)$$

where (r,θ,φ) is the polar coordinates of the point $\mathbf{x}$ viewed from the origin O, and $Y_n^m(\theta,\varphi)$ is given in the

following form using the associated Legendre function $P_n^m(x)$.

$$Y_n^m(\theta,\varphi) = \sqrt{\frac{(n-|m|)!}{(n+|m|)!}} P_n^{|m|}(\cos\theta) e^{im\varphi} \tag{17}$$

$$P_n^m(x) = \frac{1}{2^n\, n!}(1-x^2)^{\frac{m}{2}} \frac{d^{n+m}}{dx^{n+m}}(x^2-1)^n \tag{18}$$

The multipole moment M_n^{mF} of the fundamental solution, Equation (7) is given by

$$M_n^{mF} = \frac{1}{4\pi} R^n Y_n^{-m}(\theta',\varphi') \tag{19}$$

where (R,θ',φ') is the polar coordinates of the point $\mathbf{y}$ viewed from the origin O, and it is assumed that $|\overrightarrow{O\mathbf{y}}| < |\overrightarrow{O\mathbf{x}}|$.

4 Multipole moments of coefficients $A_j(x)$ and $B_j(x)$

Let the multipole moments of the coefficients $A_j(x)$ and $B_j(x)$ be M_{nj}^{mA} and M_{nj}^{mB}, respectively. The M_{nj}^{mA} and M_{nj}^{mB} for $\max_{(\mathbf{y}\in\Gamma_j)}|\overrightarrow{O\mathbf{y}}| < |\overrightarrow{O\mathbf{x}}|$ are obtained by substituting Equations (8),(16) and (19) into (10) and (11) as

$$M_{nj}^{mA} = \frac{1}{4\pi}\int_{\Gamma_j} \left\{Y_n^{-m}(\theta',\varphi')R^n\right\} d\Gamma \tag{20}$$

$$M_{nj}^{mB} = \frac{\kappa}{4\pi}\int_{\Gamma_j} \left[\nabla\left\{Y_n^{-m}(\theta',\varphi')R^n\right\}\cdot\mathbf{n}\right] d\Gamma \tag{21}$$

For the case where K elements are included in a reaf cell C, which will be defined later, the multipole moment for the cell M_{nC}^m is defined as

$$M_{nC}^m = \sum_{j=1}^{K} M_{nj}^m \tag{22}$$

where

$$M_{nj}^m = i_j M_{nj}^{mA} - \phi_j M_{nj}^{mB} \tag{23}$$

The values of M_{nj}^{mA} and M_{nj}^{mB} for a triangle constant element and a pipe element are obtained as follows; (The subscripts j will be omitted for simplicity)

4.1 Triangle constant element

By employing a coordinate system shown in Figure 1, Equations (20) and (21) are expressed as

$$M_n^{mA} = \frac{1}{4\pi}\int_{-1}^{1}\int_{-1}^{1} \left\{Y_n^{-m}(\theta',\varphi')R^n\right\} \frac{1+\xi}{4} S d\xi d\eta \tag{24}$$

$$M_n^{mB} = \frac{\kappa}{4\pi}\int_{-1}^{1}\int_{-1}^{1} \left[\nabla\left\{Y_n^{-m}(\theta',\varphi')R^n\right\}\cdot\mathbf{n}\right] \times\frac{1+\xi}{4} S d\xi d\eta \tag{25}$$

where S is the area of the triangle, and the integrand in Equation (25) is easily calculated by expressing ∇ in the following form;

$$\nabla = \mathbf{e}_R\frac{\partial}{\partial R} + \mathbf{e}_{\theta'}\frac{1}{R}\frac{\partial}{\partial\theta'} + \mathbf{e}_{\varphi'}\frac{1}{R\sin\theta'}\frac{\partial}{\partial\varphi'} \tag{26}$$

The integrals are evaluated with the Gaussian quadratures.

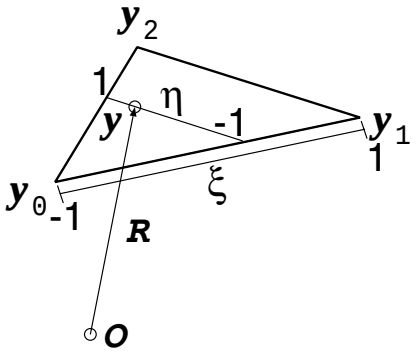

Figure 1 : Triangle element

4.2 Pipe element

By employing a coordinate system shown in Figure 2, $\mathbf{y}$ and dΓ are expressed as

$$\mathbf{y} = \frac{\mathbf{y}_2-\mathbf{y}_1}{2}\xi + \frac{\mathbf{y}_1+\mathbf{y}_2}{2} + \mathbf{a}(\alpha) \tag{27}$$

$$d\Gamma = \frac{aL}{2} d\xi d\alpha \tag{28}$$

Because the representative point of the pipe element can be taken as the center of the center line for the case of

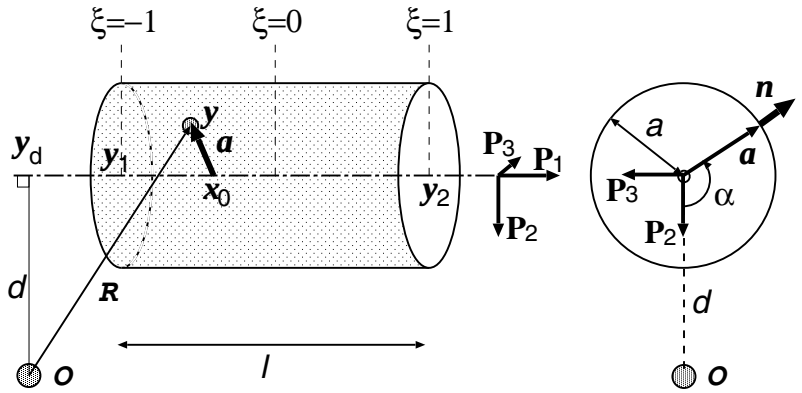

Figure 2 : Pipe element

$|\mathbf{a}|/l \ll 1$ (a: radius, l: length), the following equation holds.

$$M_n^{mA} = \frac{1}{4\pi}\int_0^{2\pi}\int_{-1}^{1}\left\{Y_n^{-m}(\theta',\varphi')R^n\right\}\frac{aL}{2}d\xi d\alpha \tag{29}$$

$$M_n^{mB} = \frac{\kappa}{4\pi}\int_0^{2\pi}\int_{-1}^{1}\left[\nabla\left\{Y_n^{-m}(\theta',\varphi')R^n\right\}\cdot\mathbf{n}\right]\frac{aL}{2}d\xi d\alpha \tag{30}$$

To evaluate the integrals, the Gaussian quadratures are used after expressing ∇ with Equation (26), as stated for the triangle element.

5 Transformation

In order to perform the fast multipole expansion it becomes necessary to shift the origin of multipole expansion, to use local expansion, and to shift the origin of local expansion. Useful formulas[Greengard (1988)] will be briefly reviewed.

5.1 Shift of the origin of multipole expansion

If the origin is shifted from O to O' in the multipole expansion, the corresponding moments are transformed as

$$\widetilde{M}_{n'}^{m'} = \sum_{n=0}^{n'}\sum_{m=-n}^{n}\frac{J_{M2M}{}_m^{m'-m}A_n^m A_{n'-n}^{m'-m}\rho^n Y_n^{-m}(\alpha,\beta)}{A_{n'}^{m'}} \times M_{n'-n}^{m'-m} \tag{31}$$

$$J_{M2M}{}_m^{m'} = \begin{cases}(-1)^{min(|m'|,|m|)}, & if\ \ m\cdot m'<0\\ 1, & otherwise\end{cases} \tag{32}$$

where

$$A_n^m = \frac{(-1)^n}{\sqrt{(n-m)!(n+m)!}} \tag{33}$$

The (ρ,α,β) stand for the polar coordinates of the old origin O viewed from the new origin O'.

5.2 Transform from multipole expansion to local expansion

The local expansion of the harmonic function $u(\mathbf{x})$ is in general expressed as

$$u(\mathbf{x}) = \sum_{n=0}^{\infty}\sum_{m=-n}^{n} L_n^m\cdot Y_n^m(\theta,\varphi)\cdot r^n \tag{34}$$

where (r,θ,φ) are the polar coodinates of the point $\mathbf{x}$ viewed from the origin of local expansion Q. Let (ρ,α,β) denote the polar coodinates of the origin of the multipole expansion O viewed from the origin of the local expansion Q. The following relationship holds between the coefficient of local expansion L_n^m and the multipole moment M_n^m.

$$L_{n'}^{m'} = \sum_{n=0}^{\infty}\sum_{m=-n}^{n}\frac{J_{M2L}{}_{n,m}^{m'}A_n^m A_{n'}^{m'}Y_{n'+n}^{m-m'}(\alpha,\beta)}{A_{n'+n}^{m-m'}\rho^{n'+n+1}}M_n^m \tag{35}$$

$$J_{M2L}{}_{n,m}^{m'} = \begin{cases}(-1)^n(-1)^{min(|m|,|m'|)}, & if\ \ m\cdot m'>0\\ (-1)^n, & otherwise\end{cases} \tag{36}$$

where A_n^m is given with Equation(33), and the inequality $|\overrightarrow{Q\mathbf{x}}| < |\overrightarrow{OQ}|$ has been assumed.

5.3 Shift of the origin of local expansion

If the origin of local expansion is shifted from Q to Q', the coefficient of the local expansion also transforms ac-

cording to

$$\tilde{L}_{n'}^{m'} = \sum_{n=0}^{p}\sum_{m=-n}^{n} \frac{J_{L2L_{n-n',m-m'}^{m}} A_{n-n'}^{m-m'} A_{n'}^{m'} Y_{n-n'}^{m-m'}(\alpha,\beta)\rho^{n-n'}}{A_n^m} L_n^m \tag{37}$$

$$J_{L2L_{n,m}^{m'}} = \begin{cases} (-1)^n(-1)^m, & if\ \ m\cdot m' < 0 \\ (-1)^n(-1)^{m'-m}, & if\ \ m\cdot m' \geq 0 \\ & \quad and\ |m'| < |m| \\ (-1)^n, & otherwise \end{cases} \tag{38}$$

where A_n^m is given with Equation (33), and (ρ,α,β) stand for the polar coodinates of the old origin Q viewed from the new origin Q'.

6 Algorithm for fast multipole expansion

The method by Greengard [Greengard (1988)] can be employed with a little modification, as shown bellow.

6.1 Determination of the octtree of cells

Discretize the finite boundary Γ given by Equation (6) into boundary elements in an ordinary manner. Take a cube circumscribing the whole Γ and call it the root cell or a cell of level 0. Then, Divide it into eight equal sub cubes and call them children cells or cell of level 1. Delete a sub cell which contains no centroid of element. If a sub cell contains a larger number of elements than a prescribed number, divide the sub cell into eight equal sub sub cubes. Otherwise, stop the division. Repeat the procedures until any division becomes impossible. Call the cell without any child cell a leaf cell.

6.2 Computation of multipole moments

(Upward Computation) Compute the multipole moment at the center of each leaf cell according to Equation (22). Then, Compute the multipole moment at the center of each parent cell by shifting the centers of children cells to that of parent one and using Equation (31). Repeat the computations until the root cell is reached.

If the whole structure to be analyzed is viewed from infinity and is assumed to be a point electric charge, it is noted from Equation (16) that the multipole moment M_0^0 is proportional to its quantity of electricity. It follows from this that an infinite domain problem can be treated by taking M_0^0 to be 0, because Equation (13) is satisfied if the quantity of electricity of a point electric charge is equal to zero.

6.3 Computation of local expansion coefficients

(Downward computation) Compute a part of the local expansion coefficient at the center of a cell of level 2 by adding the effects from the non-adjacent level 2 cells using Equation (35). Tranform this value to that at the center of the cell of level 3 (which contains the point considered) by using Equation (37). Add to it the effects from the non-adjacent level 3 cells by using Equation (35). Repeat the procedures to a leaf cell is reached, and obtain the potential $\phi(\mathbf{x})$ by using Equation (34).

The effects of cells which are not evaluated yet, i.e., those of the leaf cell which contains the point considered and the adjacent leaf cells, are calculated in an ordinary manner of the boundary element method, and are added to the above calculation result. A useful formula for this computation is available for a triangle element[Urago (2000)].

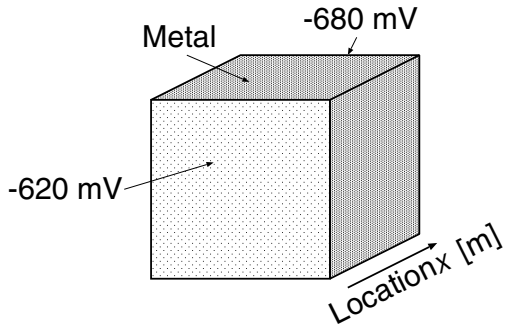

Figure 3 : Box with metal side walls, filled with electrolyte

7 Iterative procedures

The algebraic Equation (9) or (14) (Equation (15) is satisfied by taking M_0^0 to be 0, as mentioned above) can be solved by combining the fast multipole expansion and iterative procedures. However, the iterative procedures for linear equations, e.g., the Bi-CGSTAB method[Van der Vorst (1992)], have to be modified, because the polarization curve $f_m(i)$ in Equation (4) is generally non-linear. The residuals $\mathbf{r}_{q+1}$ in Bi-CGSTAB method is evaluated

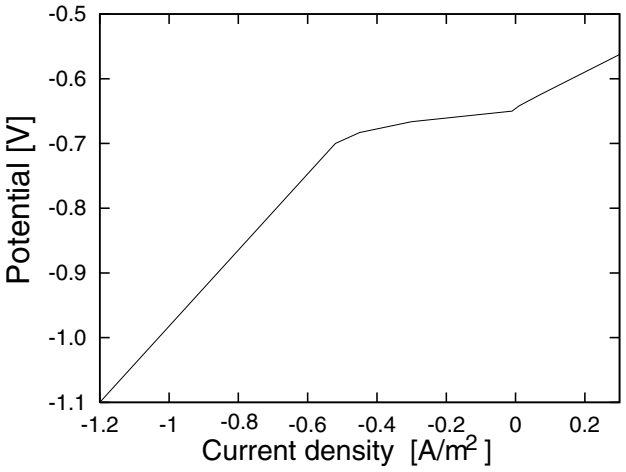

Figure 4 : Polarization curve of side wall metal

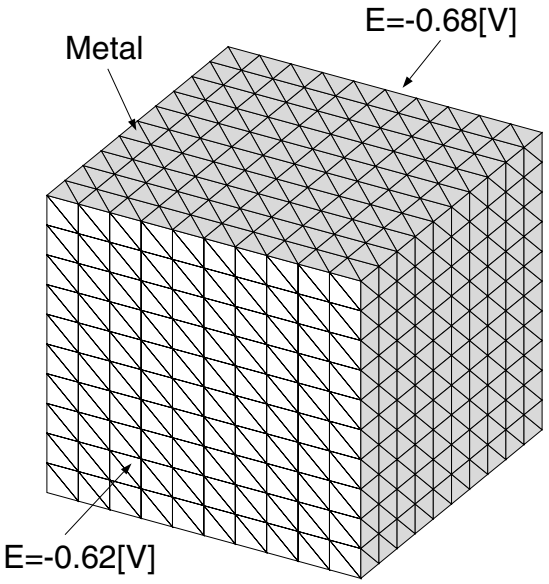

Figure 5 : Boundary element mesh for box (1200 elements)

based on linearity. In order to apply the method to non-linear equations, modify the procedures to evaluate the residuals as follows.

$$\mathbf{r}_{q+1} = \mathbf{b}(\mathbf{z}_{q+1}) - A(\mathbf{z}_{q+1})\mathbf{z}_{q+1} \tag{39}$$

where $\mathbf{z}$ is an unknown vector, $\mathbf{b}$ is a known vector, A is a non-linear matrix, the subscript (q+1) represents the number of iterations. Two sets of upward and downward calculations are necessary for one iteration in the original Bi-CGSTAB used for linear equations, while three sets of calculations become necessary for one iteration to solve non-linear equations using the above Equation (39).

8 Numerical example

8.1 Box with non-linear polarization curve

In order to verify the modified Bi-CGSTAB method in the last chapter, a box with metal side walls which is filled with electrolyte (Figure 3) was analyzed. The solution was compared with that by the ordinary boundary element method in which the Newton-Raphson iterative procedures were employed. The potential E on the right and left side walls were prescribed E =-680mV and E =-620mV, respectively. The polarization curve of the side wall metal is shown in Figure 4, and the conductivity of the electrolyte κ was κ=0.3$\Omega^{-1}m^{-1}$.

The boundary element mesh is shown in Figure 5. The maximum number L of elements in a leaf cell was assumed L=10. The terms in the multipole expansion were taken up to $n = 5$, i.e., M_{nC}^{m} in Equation (22) is assumed to be zero for $n \geq 6$.

Figure 5 compares both solutions on the potential distribution along the center line of a side wall. The FMBEM solution agrees well with the ordinary BEM solution.

Another calculation was carried out by assuming $L = 50$. The result on the potential distribution was in good agreement with that for $L = 10$ in Figure 6, while the convergence was slower as shown in Figure 7. A calculation with $L = 500$ was also performed. The solution which agreed well with that in Figure 6 was obtained at 12,000 iterations, but the residuals did not decrease smoothly.

Because the more the number of elements is allowed in a leaf, the less the cost of operation on Fast Multi-pole Method is needed, the optimum element number in a leaf may exist for corrosion problems. Further study is necessary about this problem.

For comparison, another calculation was performed under the assumption that the side walls were insulated. The solid curve in Figure 7 represents the result. A large difference in convergence between the insulated side walls and the metal ones is observed.

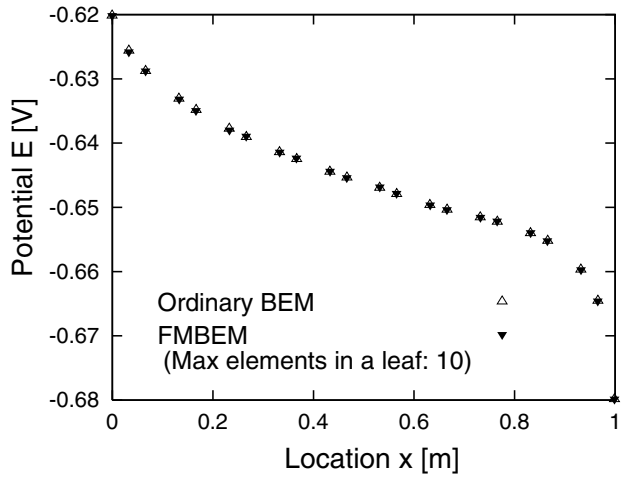

Figure 6 : Potential along center line of a side wall

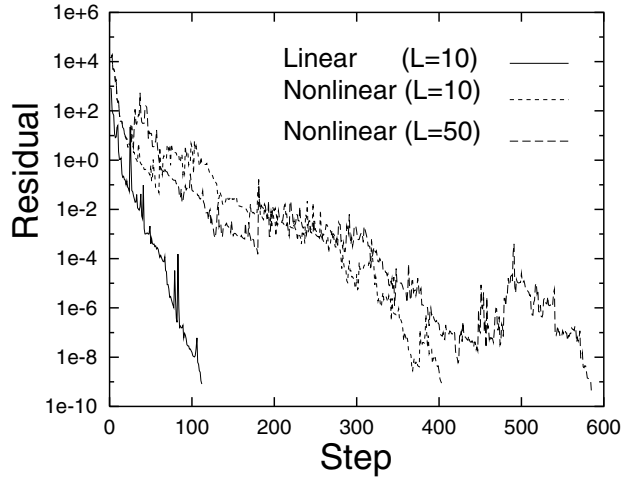

Figure 7 : Mode of convergence for box problem

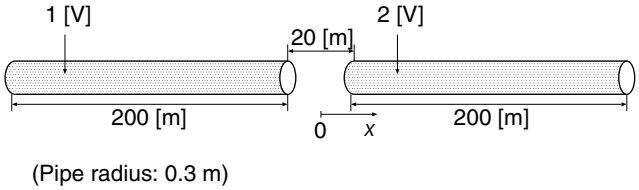

Figure 8 : Two pipes buried in infinite soil

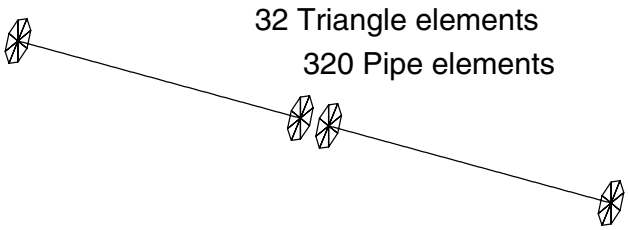

(a)Mesh of pipe elements and triangle lids

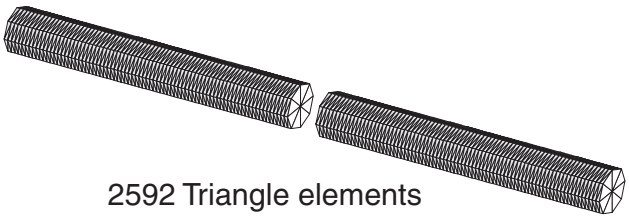

(b)Mesh of triangle elements

Figure 9 : Boundary element mesh for pipe problem

8.2 Two pipes in infinite solid

In order to verify the pipe element and the treatment of an infinite domain developed in the preceding chapters, two pipes buried in infinite soil as shown in Figure 8 were analyzed, and the results were compared with those obtained with constant triangle elements. The potential on the two pipes was assumed 1V and 2V, respectively, and no polarization was assumed. The conductivity of the soil κ was taken $\kappa = 0.3\Omega^{-1}m^{-1}$.

Figures 9(a) and 9(b) show the boundary element meshes for pipe and triangle elements, respectively. The mesh shown in Figure 9(a) where most part was discretized with pipe elements will be referred to as pipe element mesh, although a small number of triangle elements were used for the edges of the two pipes. On the other hand, the mesh shown in Figure 9(b) where every part was discretized with triangle elements will be called triangle element mesh. Figures 10 and 11 show the cell divisions for pipe and triangle elements, respectively.

For both pipe element mesh and triangle element mesh, the maximum number L of elements in a leaf cell and the terms in multipole expansion were taken $L = 10$ and $n \leq 5$, respectively. The current density distributions on the two pipes calculated with pipe and triangle elements are shown in Figure 12. Both results are in good agreement except for the edge parts of pipes.

As stated in the preceding chapter, the length l of a pipe element must satisfy the inequality $|\mathbf{a}|/l \ll 1$ (a: radius), i.e., a short pipe element can not be used. The error

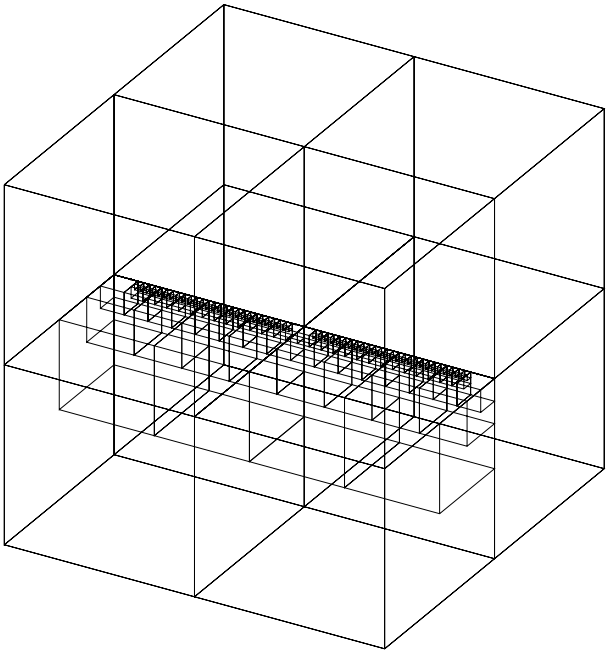

Figure 10 : FMBEM cells for pipe elements

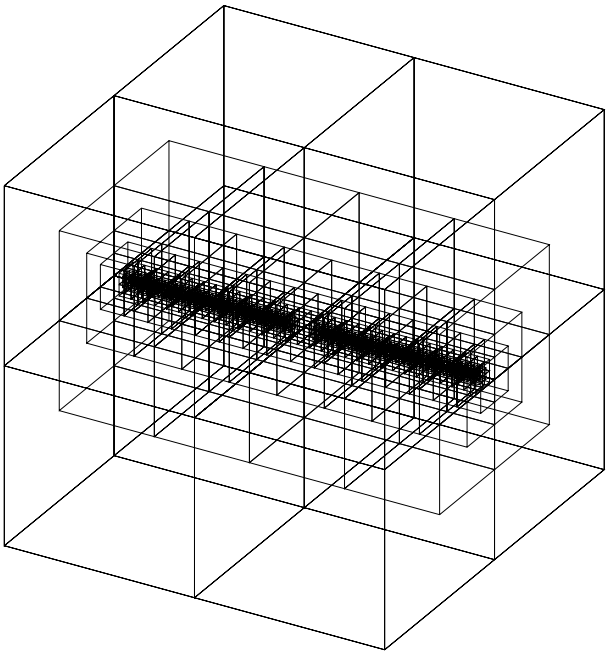

Figure 11 : FMBEM cells for triangle elements

near the edges of pipes where the current density changes steeply is attributable to this limitation of a pipe element. Figure 13 shows the convergence of the calculation. The

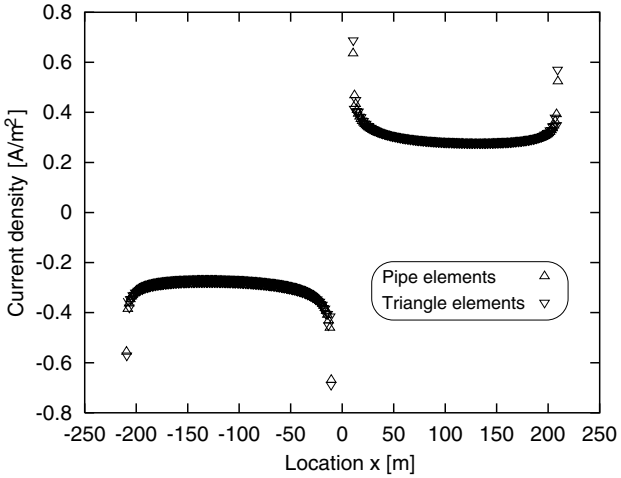

Figure 12 : Current density on pipe surfaces

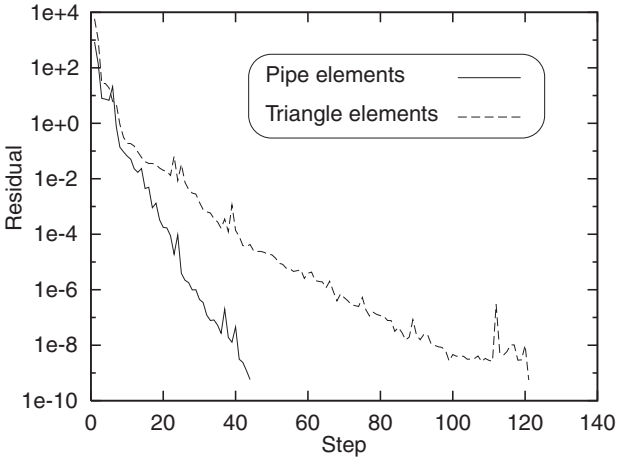

Figure 13 : Mode of convergence for pipe problem

convergence for pipe element mesh is observed more rapid than that for the triangle element mesh. It is, therefore, recommended that pipe elements should be employed for a gentle part of the field, and triangle elements should be used for a steep part.

9 Conclusions

1. Application of the fast multipole boundary element method (FMBEM) to corrosion analysis of a complicated structure was studied.

2. It was found that FMBEM can be efficiently employed by making use of many previous research results on po-

tential problems together with the following procedures.
(1) To treat an infinite domain problem, let the multipole moment M_0^0 ,which is naturally obtained in FMBEM, be zero.
(2) Modify the formula for calculating residuals in Bi-CGSTAB method, to take into account the non-linearity due to the polarization curve.
3. A pipe element suitable for the FMBEM was developed, and its characteristics were investigated.

Acknowledgement: The authors would like to express their sincere thanks to graduate student Toru Takahashi for his helpful discussion on FMBEM programming.

References

Adey, R. A.; Brebbia, C. A.; Niku, S. M. (1990): Application of Boundary Elements In Corrosion Engineering, In:C.A.Brebbia (ed.) *Topics in Boundary Element Research VII*, Springer-Verlag,Berlin, pp.34-64.

Aimi, A.; Diligenti, M.; Lunardini, F.; Salvadori, A. (2003): A New Application of the Panel Clustering Method for 3D SGBEM, *CMES: Computer Modeling in Engineering and Science*, Vol.4, No.1, pp.31-49.

Aoki, S.; Amaya, K.; Miyasaka, M. (1999): Boundary Element Analysis of Cathodic Protection for Complicated Structures, In: M.E.Orazem (ed.) *Proc. of Corrosion 99,(NACE,1999)*, pp.45-65.

Brebbia, C. A. (1978):The boundary element method for engineering, Pentech Press, London, pp.1-178.

Brichau, F.; Deconinck, J. (1994) A Numerical Model for Cathodic Protection of Buried Pipes, *Corrosion*, Vol.50, No.1, pp.39-46.

DeGiorgi, V. G.; Thomas II, E. D.; Lucas, K. E; Kee, A. (1996): A combined design methodology for impressed current cathodic protection system, In: R.C.Ertekin, C.A.Brebbia, M.Tanaka and R.Shaw(ed.) *Proc. of Boundary Element Technology XI*,Computational Mechanics Publications. Southampton, England, pp.335-344.

Fujino, K.; Chou, S. (1996): Iterative Method, Asakura,pp.1-140(in Japanese).

Fukui, T.; Hattori, J. (1998): On Numerical Evaluation of Multipole Boundary Elements in Three Dimensional Potential Problems, *Procings of 8th BEM Technology Conference*, JASCOME, Tokyo, pp.43-48(in Japanese).

Greengard, L. F.; Rokhlin, V. (1987): A Fast Algorithm for Particle Simulations, *Journal of Computational Physics*, Vol.73, pp.325-348.

Greengard, L. F. (1988):The Rapid Evaluation of Potential Fields in Particle Systems, MIT press, Cambridge, pp.1-91.

Han, Z. D.; Atluri, S. N. (2003): On Simple Formulations of Weakly-Singular Traction and Displacement BIE, and Their Solutions through Petrov-Galerkin Approaches, *CMES: Computer Modeling in Engineering and Science*, Vol.4, No.1, pp.5-20.

Hayami, K.; Sauter, S. A. (1997): Application of the panel clustering method to the three-dimmensional elastostatic problem, In: C.A.Brebbia and M.H.Aliabadi (ed) *Boundary Elements XIX*, Computational Mechanics Publications,Southampton, England, pp.625-634.

Nishimura, N.; Yoshida, K.; Kobayashi, S. (1999): A Fast Multipole Boundary Integral Equation Method for Crack Problems in 3D, *Engineering Analysis with Boundary Elements*, Vol.23, pp.97-105.

Orazem, M. E.; Esteban, J. M.; Kennelley, K. J.; Degerstedt, R. M. (1997): Mathematical Models for Cathodic Protection of an Underground Pipeline with Coating Holidays: Part 1 – Theoretical Development, In: *Corrosion*, Vol.53, No.4, pp.264-272.

Rokhlin, V. (1987): Rapid Solution of Integral Equations of Classical Potential Theory, *Journal of Computational Physics*, Vol.60, pp.187-207.

Takahashi, T.; Nishimura, N.; Kobayashi, S. (2001): Fast Boundary Integral Method for Elastodynamic problems in 2D in Time Domain, *Transactions of Japan Soc. Mech. Eng.*, Vol.67A, No.661, pp.1409-1416 (in Japanese).

Urago, M.(2000):Analytical Integrals of Fundamental Solution of Three-Dimensional Laplace Equation and Their Gradients, *Transaction of Japan Soc. Mech.Eng.*, Vol.66A, No.642, pp.254-261 (in Japanese).

Van der Vorst, H. A. (1992): Bi-CGSTAB: a fast and smoothly converging variant of Bi-CG for the solution of nonsymmetric linear systems, *SIAM J. Sci. Stat. Comput.*, Vol.13, pp.631-644.